

# Properties of ZnO and ZnMnO Thin Films Obtained by Pulsed Laser Ablation

I.S. VIRT<sup>a,c</sup>, I.V. HADZAMAN<sup>a</sup>, I.S. BILYK<sup>a</sup>, I.O. RUDYI<sup>c</sup>, I.V. KURILO<sup>c</sup>,  
M.S. FRUGYNSKYI<sup>c</sup> AND P. POTERA<sup>b</sup>

<sup>a</sup>Drogobych State Pedagogical University, I. Franko st., 24, 82100 Drogobych, Ukraine

<sup>b</sup>Rzeszów University, Rejtana 16A, 35-310 Rzeszów, Poland

<sup>c</sup>Lviv Polytechnic National University, Bandera st., 12, 79013 Lviv, Ukraine

The results of experimental investigation of structural and physical properties of ZnO and ZnMnO films are presented in this work. The films of ZnO and Zn<sub>1-x</sub>Mn<sub>x</sub>O of different thickness were obtained on Al<sub>2</sub>O<sub>3</sub>, glass, and KCl substrates in vacuum of  $1 \times 10^{-5}$  Torr by the pulsed laser deposition method. The samples were obtained under the substrate temperature 300–473 K. A thickness of films was in the range of 0.5–1  $\mu\text{m}$  depending on the number of laser pulses. The structure of target bulk materials was investigated by X-ray diffraction method. A structure of laser deposited films was investigated by the transmission high-energy electron diffraction method. Electric resistivity was measured in the temperature range 77–450 K. The presence of two activation energies in the temperature range 300–330 K and 330–450 K is followed from the analysis of the films electrical resistivity. These activation energies correspond to two deep donor's energy levels. The shallow donor's level is connected with manganese presence. Optical transmission of ZnO and ZnMnO films deposited at various temperatures were investigated.

PACS numbers: 81.05.Dz, 81.15.Fg, 72.80.Ey, 78.20.Ci

## 1. Introduction

Zinc oxide is a wide gap II–VI semiconductor material which attracts attention of researchers in different areas. This semiconductor has several favorable properties: good transparency, high electron mobility, wide band gap, strong room-temperature luminescence, etc. Those properties are already used in emerging applications for transparent electrodes in liquid crystal displays and in energy-saving or heat-protecting windows and as thin-film transistor and light-emitting diode. The special attention is given to the investigation of thin film materials and structures on their basis, especially those which are doped with magnetic impurities. ZnO films is a promising material for optoelectronics, spintronics and sensor technology [1–3].

In the given work results of experimental research of structural and physical properties of ZnMnO thin films are presented. Thin films were deposited by a method of pulsed laser ablation of targets Zn<sub>1-x</sub>Mn<sub>x</sub>O ( $x \approx 0.08$ ). The good stoichiometry of films was achieved due to special methods of targets preparation.

## 2. Experimental details

### 2.1. Sample preparation

The ZnO and Zn<sub>1-x</sub>Mn<sub>x</sub>O films were prepared by the pulsed laser ablation (PLA) method which is very

prospective for fabrication of thin films. The most important practical advantages of this method are: low substrate temperature, good adhesion, high deposition rate, a relatively wide energy range of particles (1–1000 eV). A simplicity of PLA technique was successfully applied for II–VI compounds such as CdTe, HgCdTe, CdS, ZnS, and ZnTe [4, 5].

The targets were prepared by the preliminary grinding and the subsequent sintering of ZnO and also ZnO powders with addition of Mn (Zn<sub>1-x</sub>Mn<sub>x</sub>O,  $x = 0.04$ ). The Zn<sub>1-x</sub>Mn<sub>x</sub>O powder was formed as a result of reactions:  $\text{MnCO}_3 + \text{ZnO} \rightarrow \text{ZnO} + (\text{MnO})_{1-x} + (\text{Mn}_2\text{O}_3)_x + \text{CO}_2 \uparrow$ ;  $\text{ZnO} + \text{MnO} \rightarrow \text{Zn}_x\text{Mn}_{1-x}\text{O}$ . The MnCO<sub>3</sub> powder was mixed with ZnO powder and sintered at 973 K and 1383 K.

For removing of the target material the YAG:Nd<sup>3+</sup> laser ( $\lambda = 1064$  nm, pulse width  $\Delta t = 10$  ns and frequency  $f = 0.5$  s<sup>-1</sup>) was used. The films were deposited from target on the glass, Al<sub>2</sub>O<sub>3</sub> (0001) and KCl (001) substrates at various temperatures ( $T_s = 300$ –473 K) and various operating modes of the laser.

It is established that thickness of the films obtained by PLA from ZnMnO targets is a little bit greater than those ones obtained from ZnO targets.

### 2.2. Measurement techniques and procedure

A structure of the bulk materials of target was investigated by X-ray diffraction (XRD) method in the

$\theta$ - $2\theta$  configuration. A structure of laser deposited films was investigated by the transmission high-energy electron diffraction (HEED) method using an EG-100 electron-graph with 80 kV accelerator. Electric parameters were determined by the two-probe method. The temperature measurements of resistivity were made with "Metex" electrometer and Keithley thermocouple meter. The upper limit of the temperature measurements was 450 K. The measurements of the films optical transmittance and reflectance were carried out by the UNICAM UV 300 spectrometer.

### 3. Results and discussion

#### 3.1. Structural properties

The  $d$ -value of each peak in the diffraction pattern is compared with JCPDS standard  $d$ -values for ZnO and MnO<sub>2</sub> [6]. Table I shows the comparison of observed for ZnO and Zn<sub>1-x</sub>Mn<sub>x</sub>O  $d$ -values with the standard  $d$ -values. The indices of all the peaks on XRD and HEED pattern are identified. The structure of the bulk alloy is hexagonal and the lattice constants  $a$  and  $c$  have been calculated and are found to be  $a = 3.2479$  Å,  $c = 5.2029$  Å of ZnO and  $a = 3.2518$  Å,  $c = 5.2072$  Å of Zn<sub>1-x</sub>Mn<sub>x</sub>O.

TABLE I

Comparison of  $d$ -values of ZnO, Zn<sub>1-x</sub>Mn<sub>x</sub>O ( $x = 0.04$ ) bulk and thin films from XRD and HEED data with standard  $d$ -value from ZnO, MnO<sub>2</sub>.

JCPDS values (ASTM)		Observed $d_{hkl}$ values [Å]				
$d_{hkl}$ [Å]		XRD (bulk)			HEED (films)	
ZnO	MnO <sub>2</sub>	ZnO	Zn <sub>1-x</sub> Mn <sub>x</sub> O	$hkl$	ZnO	Zn <sub>1-x</sub> Mn <sub>x</sub> O
–	4.2150	–	4.2961	101	–	–
2.8143	–	2.8128	2.8162	100	–	2.851
2.6033	2.67320	2.6014	2.6036	002	–	2.628
2.4659	2.4550	2.4741	2.4775	101	–	–
1.9111	1.9380	1.9099	1.9124	102	1.925	1.940
1.6247	1.6375	1.6242	1.6269	110	1.642	1.608
1.4771	1.4320	1.4764	1.4783	103	1.483	–
1.3782	1.3604	1.3778	1.3799	112	–	–

The HEED patterns from ZnO and Zn<sub>1-x</sub>Mn<sub>x</sub>O thin films (Fig. 1a) obtained at  $T_s = 300$  K showed some diffuse polycrystalline rings. An average size of particles was about 50 Å. The HEED patterns (Fig. 1b) from Zn<sub>1-x</sub>Mn<sub>x</sub>O thin films obtained at  $T_s = 473$  K indicate on the polycrystalline structure which is formed by the particles with average sizes of 400 Å.

The mean size of particles can be estimated from a diffuseness of the diffraction ring by using the Scherrer formula [7]:

$$L = 0.9\lambda/B \cos \theta_B, \quad (1)$$

where  $L$  is the mean particles size,  $\lambda$  is the wavelength

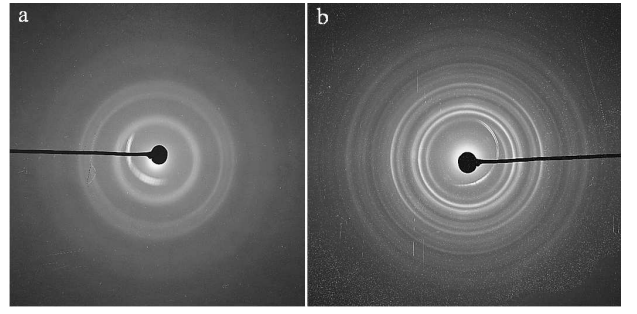


Fig. 1. HEED patterns of thin films: ZnO ( $T_s = 300$  K) (a), Zn<sub>1-x</sub>Mn<sub>x</sub>O ( $T_s = 473$  K) (b).

of the electron beam,  $B$  is half-width of ring broadening,  $\theta_B$  is diffraction angle. The Scherrer formula with single-error corrections on length of a wave and geometry in conditions of a electron diffraction is used [8].

#### 3.2. Electrical properties

The resistivity dependences of ZnO films in  $\ln \rho - 1/T$  coordinates are shown in Fig. 2. The two intervals on temperature dependences were observed: low-temperature (300–330 K) and high-temperature (330–450 K). The decrease of films resistivity corresponds to the linear temperature function and indicates semiconductive properties of ZnO.

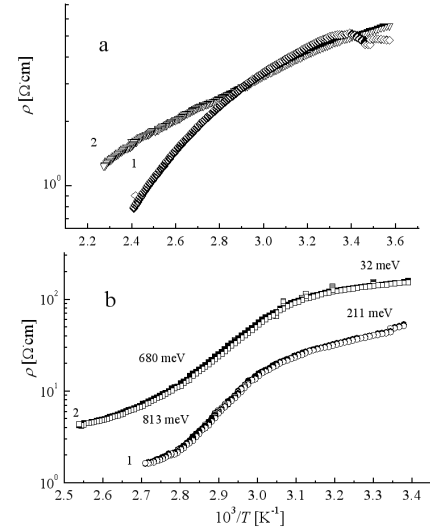


Fig. 2. Temperature dependence of the resistivity of the films: Zn<sub>1-x</sub>Mn<sub>x</sub>O ( $x = 0.04$ ) (a),  $T_s = 300$  K (1),  $T_s = 470$  K (2); ZnO (1), Zn<sub>1-x</sub>Mn<sub>x</sub>O (2),  $T_s = 470$  K (b).

Thus the activation energy  $\Delta E$  was calculated from formula

$$\rho = \rho_0 e^{\Delta E/kT}, \quad (2)$$

where  $\rho$  is conductivity,  $\rho_0$  is constant,  $k$  is the Boltzmann constant,  $T$  is temperature.

From the slope of curves  $\ln \rho - 1/T$  the activation energy was calculated (Fig. 2b).

The analysis of temperature dependences of resistivity of the film testifies that for all the films two activation energies in various temperatures intervals are characteristic (Fig. 2). The values of these energies were different for different composition. The analysis testifies the existence of two deep energy levels (0.68–0.81 and 0.21 eV). The shallow donor level (0.03 eV) becomes apparent at the presence of manganese. Rather low resistivity was observed in low thickness films (less than 100 nm). Let us notice that measurements of these films were carried out directly during their growth (*in situ*). It was established that with the increase of film thickness the growth rate decreases. It indicates on better adhesion of Zn atoms at the initial stages of film growth.

It is known that the insufficiency of oxygen is typical for ZnO films obtained by various techniques. As a result these films have low specific resistance [2]. However, ZnO film obtained by PLA method possesses rather high electric resistance. It can be explained with the influence of oxygen chemisorption during sedimentation. It should be noted that concentration of oxygen in the chamber can be adjusted by residual pressure of gases. It is known that during the deposition process a large number of oxygen molecules are chemically adsorbed on grain boundaries as well as on film surface. The excessive oxygen molecules have no time to leave a film at the end of growth process due to its rapid cooling. During the heating the oxygen molecules evaporate from the sample. It results in the decrease of resistivity as it was observed experimentally.

The temperature dependences of resistivity were also measured during samples cooling. A hysteresis phenomenon was observed in all the samples. The cooling curves  $\ln \rho - 10^3/T$  are situated higher as compared to the heating ones.

### 3.3. Optical properties

The optical transmission spectra of ZnO and  $\text{Zn}_{1-x}\text{Mn}_x\text{O}$  films grown at various temperatures are presented in Fig. 3. The significant decrease of transmittance observed in the ultraviolet region is due to a band-to-band transition. The shift of the absorption edge to higher energies is proportional to the substrate temperature as it follows from corresponding absorption spectra (Fig. 3b).

The analysis of optical spectra of ZnO films showed the existence of direct interband gap in the obtained thin films. The optical width of ZnO films energy band for direct transitions has been determined from

$$\alpha h\nu = A\sqrt{h\nu - E_g}, \quad (3)$$

where  $A$  is a constant.

The values of optical width of the forbidden zone were evaluated using the absorption spectra for ZnO and  $\text{Zn}_{0.92}\text{Mn}_{0.08}\text{O}$  films obtained at various surface temperatures and are given in Table II. As it can be seen, the value of  $E_g$  closest to a bulk material is characteristic for ZnO film. The addition of manganese in ZnO results in

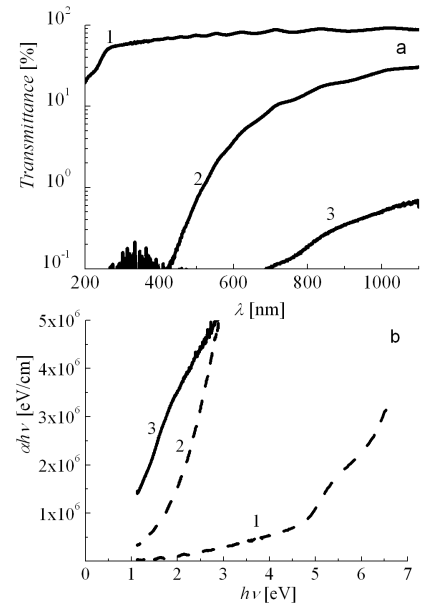


Fig. 3. The optical spectra of thin films: (a) transmittance spectra for ZnO,  $T_s = 470$  K (1),  $\text{Zn}_{1-x}\text{Mn}_x\text{O}$ ,  $T_s = 300$  K (2),  $\text{Zn}_{1-x}\text{Mn}_x\text{O}$ ,  $T_s = 470$  K (3); (b) absorption spectra for ZnO,  $T_s = 470$  K (1),  $\text{Zn}_{1-x}\text{Mn}_x\text{O}$ ,  $T_s = 300$  K (2),  $\text{Zn}_{1-x}\text{Mn}_x\text{O}$ ,  $T_s = 470$  K (3).

a shift of absorption edge in long wavelength region of a spectrum. Similar long wavelength optical shift was observed in [9] at introduction of transitive metals to ZnO, in particular cobalt. Authors connect such shift with the increase of *sp-d* type exchange interaction.

TABLE II

Optical width of the forbidden zone for the ZnO and  $\text{Zn}_{0.92}\text{Mn}_{0.08}\text{O}$ .

Films	$E_g$ [eV]
ZnO, $T_s = 200^\circ\text{C}$	4.05
$\text{Zn}_{0.92}\text{Mn}_{0.08}\text{O}$ , $T_s = 30^\circ\text{C}$	1.74
$\text{Zn}_{0.92}\text{Mn}_{0.08}\text{O}$ , $T_s = 200^\circ\text{C}$	0.72
bulk ZnO	3.37

## 4. Conclusions

The structural, electric and optical properties of ZnO and  $\text{Zn}_{1-x}\text{Mn}_x\text{O}$  films obtained by PLA were investigated. The average sizes of particles of polycrystalline ZnO and  $\text{Zn}_{1-x}\text{Mn}_x\text{O}$  obtained at 300 K and  $\text{Zn}_{1-x}\text{Mn}_x\text{O}$  films obtained at 473 K were evaluated by means of HEED method as 50 Å and 400 Å, correspondingly.

The ZnO and  $\text{Zn}_{1-x}\text{Mn}_x\text{O}$  film possess rather high electric resistance that is connected with influence of oxygen chemisorption during sedimentation.

The values of activation energy in various temperature intervals (0.68–0.81 and 0.21 eV) have been determined from the temperature dependences of the films specific resistance. The films containing manganese revealed shallow donor level (0.03 eV) as well. The values of these energies depend on the composition of films. The films with thickness smaller than 100 nm possess low specific resistance. The measurements of temperature dependences of specific resistance in heating and cooling modes showed hysteresis behavior.

The addition of manganese in ZnO results in the shift of absorption edge to the long wavelength region of spectrum. This phenomenon is similar to the red shift of the optical width of forbidden zone at introduction of transitive metals in ZnO. The shift of the absorption edge to higher energy region is proportional to the temperature of substrate. From the absorption spectra of ZnO and Zn<sub>0.92</sub>Mn<sub>0.08</sub>O films obtained at various substrate temperatures the values of optical forbidden zone width have been determined.

## References

- [1] Ü. Özgür, Ya.I. Alivov, C. Liu, A. Teke, M.A. Reshchikov, S. Doğan, V. Avrutin, S.-J. Cho, H. Morkoç, *J. Appl. Phys.* **98**, 041301 (2005).
- [2] V. Khranovskyy, J. Eriksson, A. Lloyd-Spetznita, R. Yakimova, L. Hultman, *Thin Solid Films* **517**, 2073 (2009).
- [3] I. Lorite, F. Rubio-Marcos, J.J. Romero, J.F. Fernández, *Mater. Lett.* **63**, 212 (2009).
- [4] I.S. Virt, M. Bester, L. Dumański, M. Kuźma, I.O. Rudyi, M.S. Frugynskyi, I.V. Kurilo, *Appl. Surf. Sci.* **177**, 201 (2001).
- [5] P. Sagan, G. Wisz, M. Bester, I.O. Rudyj, I.V. Kurilo, I.E. Lopatynskij, I.S. Virt, M. Kuzma, R. Ciach, *Thin Solids Films* **480-481**, 318 (2005).
- [6] *Joint Committee on Powder Diffraction Standards (JCPDS) diffraction data card*, American Society for Testing and Materials (ASTM).
- [7] B.D. Cullity, *Elements of X-ray Diffraction*, 2nd ed., Addison-Wesley, Reading, MA 1978, pp. 284, 366.
- [8] Z.G. Pinsker, *Electron Diffraction*, Butterworths Sci. Publ., London 1953.
- [9] Y. Belghazi, M.A. Aouaj, M. El Yadari, G. Schmerber, C. Ulhaq-Bouillet, C. Leuvrey, S. Colisa, M. Abd-lefdil, A. Berrada, A. Dinia, *Microelectron. J.* **40**, 265 (2009).